Journal of Materials Chemistry B

Unique Sequence-Dependent Properties of Trinucleotide Repeat Monolayers: Electrochemical, Electrical, and Topographic Characterization

Journal:	*Journal of Materials Chemistry B*
Manuscript ID	TB-ART-02-2020-000507.R1
Article Type:	Paper
Date Submitted by the Author:	30-Apr-2020
Complete List of Authors:	Asefifeyzabadi, Narges; Southern Illinois University Carbondale, Chemistry and Biochemistry Taki, Motahareh; Southern Illinois University System, Chemistry Funneman, Madison; Southern Illinois University Carbondale, Chemistry and Biochemistry Song, Tingjie ; University of Illinois at Urbana-Champaign, Chemistry Shamsi, Mohtashim; Southern Illinois University, Chemistry and Biochemistry

Unique Sequence-Dependent Properties of Trinucleotide Repeat Monolayers: Electrochemical, Electrical, and Topographic Characterization

Narges Asefifeyzabadi,[a] Motahareh Taki,[a] Madison Funneman,[a] Tingjie Song,[b]

and Mohtashim Hassan Shamsi[a]*

[a] Department of Chemistry & Biochemistry, 1245 Lincoln Dr, Southern Illinois University at Carbondale, IL 62901, USA. [b] Department of Chemistry, University of Illinois at Urbana-Champaign, IL 61801, USA.

*mshamsi@siu.edu

1. Abstract.

Trinucleotide repeat (TNR) sequences widely exist in nature and their overgrowth is associated with two dozen neurodegenerative diseases in humans. These sequences have unique helical flexibility which affects their biophysical properties. Number of biophysical properties of these sequences have been studied in the past except their surface-tethered monolayers. To address the effect of sequence context and the associated helical flexibility on TNR monolayers, disease-relevant TNRs from three flexibility groups were surface-assembled on gold surfaces. The properties of the TNR films including charge transfer resistance (R_{ct}) was studied by electrochemical impedance spectroscopy (EIS), surface density by chronocoulometry (CC), surface topography by atomic force microscopy (AFM), and electrical conductivity by conducting atomic force microscopy (C-AFM). We found that the TNR film properties are characteristically sequence dependent rather than their flexibility rank reported in the literature. The characteristic properties of TNR films studied here will be used engineering label-free biosensors to detect neurological disorders and build DNA bioelectronics.

2. Introduction.

DNA repeat sequences such as trinucleotide repeat (TNR) is a class of short nucleic acid sequences that repeat sporadically and in tandem across living organisms. In humans, some TNRs have been associated with over two dozen genetically transferrable neuromuscular and neurodegenerative diseases.[1-2] At molecular level, the repetition of TNR combinations leads to certain sequence-directed flexibility that allows them to form unique secondary structures.[3-4] Theoretical calculations based on helical parameters have classified 64 possible TNR combinations into 12 groups of flexibilities.[5] In contrast to a random sequence, the persistence lengths of some TNRs were reported 40% lower than normal B-DNA having 50 nm persistence length.[6] Moreover, presence of only four TNR repeats in a sequence may introduce a flexibility in helical structure similar to flexibility caused by a dinucleotide T-T mismatch.[7]

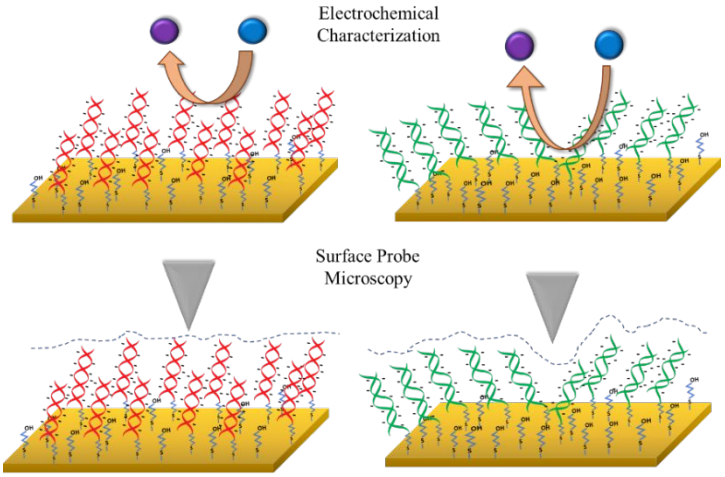

Scheme 1. Depicting electrochemical and surface probe microscopic characterization of self-assemblies of rigid and flexible TNR sequences on gold surfaces. The TNR sequences were tethered to gold surfaces through Au-S$(CH_2)_6$-DNA linkage and nonspecific binding was prevented by filler layer of mercaptohexanol (MCH).

A few disease specific TNRs (CGG, CTG, CAG, and GAA) have been widely characterized by a range of techniques including electrophoresis,[8-9] mass spectroscopy,[10] circular dichroism,[11] nuclear magnetic resonance,[12-13] optical melting study and differential scanning calorimetry,[14-15] and recently by a pump-free wax-on-plastic microfluidics.[16] Nevertheless, TNR-based biointerfaces have not been characterized thus far. For biosensing and bioelectronic applications, the knowledge of DNA-based interfaces or surface-assembled films are critical such as surface densities, charge transport properties, electrostatics, molecular mechanics, stability of surface-tethered states, and interactions with surface and neighbouring environment.[17]

Here, we first time report a systematic study on TNR surface-tethered monolayers. As depicted in **Scheme 1**, surface-tethered films may assume unique monolayers owing to their sequence-directed helical parameters that may translate into unique electrochemical and surface-probe signals. To investigate the effect, we characterize the monolayers of three TNR sequences from three different flexibility groups on gold surfaces. The surface properties that were studied include charge transfer resistance (R_{ct}) by electrochemical impedance spectroscopy (EIS), surface density by chronocoulometry (CC), surface topography by atomic force microscopy (AFM), and electrical conductivity by conducting atomic force microscopy (C-AFM). The evidence of unique film properties of TNR evolved from this study reinforces the efforts of developing label-free biosensors to detect DNA repeat expansion disorders and developing bioelectronic devices.[18]

3. Experimental.

3.1. Reagent and Materials.

$K_4[Fe(CN)_6]$, $K_3[Fe(CN)_6]$, sulfuric acid (98%), and sodium chloride were purchased from Thermo Fisher Scientific (Waltham, MA). Tris(hydroxymethyl)aminomethane (Tris-ClO_4),

$Ru(NH_3)_6Cl_3$, 6-Mercapto-1-hexanol (MCH) and magnesium chloride solution (1 M) were purchased from Sigma-Aldrich (St. Louis, MO). Gold disc electrodes and platinum wire electrodes were purchased from CH Instruments (Bee Cave, TX). The Ag/AgCl reference electrodes and velvet cloth to polish electrodes were obtained from Bioanalytical Systems Inc. (West Lafayette, IN). The HPLC purified probe sequences with a 6-hydroxyhexyl disulfide group at 5' position and the complementary sequences were purchased from IDT (Integrated DNA Technologies, Coralville, IA). Template-Stripped ultra-flat gold substrates were purchased from Platypus Technologies. Olympus tips, AC240TM with platinum coating was used for topographic and conductivity measurements of atomic force microscopy (AFM).

3.2. Preparation of TNR Solutions.

To prepare 10 μM double-stranded TNR solutions, 20 μL aliquots of 20 μM $OH(CH_2)_6$-S-S-$(CH_2)_6$-modified base sequence and 20 μM of complementary sequences were mixed in a buffer (100 μM Tris buffer containing 20 mM $MgCl_2$ and 200 mM NaCl) with pH 8.5 and heated up to melting temperatures of TNRs for 30 minutes followed by annealing to room temperature for 1 hour and stored at 4 ^oC.

3.3. Preparing Surface-Tethered Films of TNRs on Gold Electrodes.

For electrochemical study, surfaces of gold working electrodes were regenerated by mechanical and electrochemical polishing. Briefly, gold disc electrodes of 2 mm diameter were polished with three different grain sizes of alumina powder (1, 0.3, and 0.05 μm) followed by 10 minutes sonication in DI water. Cyclic voltammetry was performed for electrochemical cleaning of the mechanically polished electrodes by running 20 cycles in 0.5 M H_2SO_4 with a potential range of 0–1.5 V against an Ag/AgCl reference electrode and a platinum wire counter electrode. The gold oxide stripping peak of the last cycle was used to measure the roughness factor of the

electrodes that was kept ≤ 1.2. The electrodes were preserved in 1:1 ethanol: water mixture. Then, 10 μL of hybridized solutions of TNRs were dropped on the electrodes to form films on the freshly cleaned and polished gold surfaces at 4 °C. The electrodes were capped with Eppendorf tubes to prevent evaporation and incubated for 4 days according to our optimized condition,[18] where the disulfide bond in the presence of gold breaks into thiol group spontaneously and attach to gold surface through Au-S linkage.[19] Then, the modified electrodes were washed with buffer and further incubated in 1 mM mercaptohexanol for 30 minutes to block any unbound surface of the gold electrode and remove physically adsorbed DNA strands followed by another washing step.

3.4. Electrochemical Measurements.

All electrochemical experiments were performed by CHI 660E (CHI, Austin, TX) at room temperature in a three-electrode cell with the modified gold electrodes as the working electrode (with the geometric area of 0.0314 cm^2), platinum wire counter electrode and Ag/AgCl reference electrode. Electrochemical impedance spectroscopy (EIS) was carried for double-stranded repeat sequences using soluble redox probe, i.e. 1 mM $[Fe(CN)_6]^{3-/4-}$ prepared in 100 μM of Tris buffer pH 7.4. The following parameters were used to run the EIS measurements: Frequency range from 100 kHz to 1 Hz, an applied potential of 250 mV vs. Ag/AgCl, and AC voltage of 5 mV amplitude. For simulation, Z-view version 3.5d was used to fit the EIS data into Randle's equivalent circuit and to extract the values for charge transfer resistance (R_{ct}).

Tarlov's method was used to calculate surface density of TNR using chronocoulometry.[20] Briefly, this involves charge measurement on DNA modified electrode surfaces before and after exposure of DNA films to $Ru(NH_3)_6^{3+}$. In chronocoulometric study, a potential step was applied to the TNR modified electrodes followed by measuring resulting charge vs. $(time)^{1/2}$ under

equilibrium condition in the absence and presence of 5 μM [Ru $(NH_3)_6]^{3+}$ prepared in 10 mM Tri-ClO_4 (pH 7.4). The chronocoulometric measurements were carried out with the pulse period of 500 ms, pulse width of 600 mV (from +150 mV to -450 mV) and quiet time of 30 s. Deoxygenation of the solution was performed by purging the nitrogen gas through the buffer and redox marker solution for 30 minutes before measurement. Representative plots of CC measurements are shown in the **Figure S1** in the supplementary information.

3.5. Atomic Force Microscopy and Conductivity Measurements.

Ultra-flat gold substrates were used for all AFM measurements and were washed with acetone and deionized water followed by rinsing with Tris buffer and finally drying under N_2. Then, 10 μM double-stranded TNR solutions as prepared above were dropped on the surfaces of clean gold substrates and incubated as mentioned above. Then, the surfaces were rinsed with the Tris buffer and dried under N_2 before AFM measurements. All AFM measurements were performed in air dry condition using Cypher S Asylum Research AFM Microscope, at University of Illinois Urbana-Champaign, in air (dry). Olympus tips, with platinum coating, spring constant 2 N/m, resonance frequency 70 kHz and tip radius 15 nm were used. Open source imaging analysis software 'Gwyddion' was used for analysing the AFM images.[21] Topographic images with resolutions of 300 nm × 300 nm and 1 μm × 1 μm area were obtained using tapping mode in three replicate surfaces. The surface profiles were extracted from the images across centre of each image. For electrical measurements by AFM, sample was mounted on AFM disc and Leitsilber silver paint was used to conductively glue the sample on AFM disc. The conductivity measurements were made in contact mode, where the electrically conductive probe was scanned over the DC-biased TNR-modified surfaces. The current-potential (*I-V*) curves were obtained by single point measurement of the current as a function of voltage applied to the sample. Before running current-

voltage curves, an image was collected from the sample surface in AC mode and then changing over to contact mode and collecting the spectra from the chosen spots. The setpoint potential of 0.1–0.5 V corresponding to 17–85 nN applied force were used to collect *I-V* curves between ±2 V applied potential.

Table 1. Description of the trinucleotide repeats with their complementary sequences.

TNR type	Sequence[a]	Repeat Length	Flexibility[b]
CGG-8	5'linker- CGG CGG CGG CGG CGG CGG CGG CGG -3' 3'- GCC GCC GCC GCC GCC GCC GCC GCC -5'	8	Highly Flexible
CCG-8	5'linker- CCG CCG CCG CCG CCG CCG CCG CCG -3' 3'- GGC GGC GGC GGC GGC GGC GGC GGC -5'	8	
CAG-4	5'linker- CAG CAG CAG CAG-3' 3'- GTC GTC GTC GTC-5'	4	Medium Flexible
CAG-8	5'linker- CAG CAG CAG CAG CAG CAG CAG CAG -3' 3'- GTC GTC GTC GTC GTC GTC GTC GTC -5'	8	
CTG-8	5'linker- CTG CTG CTG CTG CTG CTG CTG CTG -3' 3'- GAC GAC GAC GAC GAC GAC GAC GAC -5'	8	
GAA-4	5'linker- GAA GAA GAA GAA-3' 3'- CTT CTT CTT CTT-5'	4	Least Flexible
GAA-5	5'linker- GAA GAA GAA GAA GAA-3' 3'- CTT CTT CTT CTT CTT-5'	5	
GAA-8	5'linker- GAA GAA GAA GAA GAA GAA GAA GAA -3' 3'- CTT CTT CTT CTT CTT CTT CTT CTT -5'	8	

[a]Linker molecule $OH(CH_2)_6$-S-S-$(CH_2)_6$-DNA. The disulfide bond in the presence of gold breaks into thiol group spontaneously and attach to gold surface through Au-S linkage Ref. [22].

4. Results and Discussion.

Based on computational analysis of helical parameters, Baldi *et al.* classified 64 possible TNR sequences into 12 groups by designating a value to each TNR on so-called 'flexibility scale'.[5] According to the computational model, the TNRs given in **Table 1** are ranked in flexibility CGG > CTG > GAA. While, another report ranked these sequences as CTG > CGG ≈ GAA.[22] In this study, the prehybridized TNR duplexes were surface-tethered on cleaned and polished gold surfaces through Au–S linkage followed by filling the residual space with mercaptohexanol (MCH) to prevent nonspecific adsorption of nucleobases on gold surfaces. First, the TNR-modified gold electrodes were characterized by EIS, which has been extensively used as label-free

macroscopic approach to detect structural distortion in DNA at molecular level that manifests into distinct monolayers.[23-27] EIS was used to test the diffusion of a soluble redox probe, $Fe(CN)_6^{3-/4-}$, through the TNR films where the diffusion is impeded by the electrostatic repulsion between the redox probe and negatively charged phosphate backbone of DNA along with physical resistance of the film. The EIS data was fit into modified Randle's equivalent circuit (see **Figure S2** in supplementary information). The resistive and capacitance elements were extracted by fitting the experimental data into modified Randle's equivalent circuit given in **Table 2**. Among all the circuit element charge transfer resistance (R_{ct}) was found to be a distinctive property with lower standard error (RSD ~10%) across the sequences, thus, it was used to compare the sequences in **Figure 1**.

Table 2. The average values of modified Randle's equivalent circuit elements for each double-stranded TNR sequence. The standard errors in parentheses were calculated for N ≥ 4 separate measurements.

	R_s $\Omega \cdot cm^2$	C_{dl} $F \cdot cm^{-2}$ (10^{-8})	R_{ct} $\Omega \cdot cm^2$	W $\Omega \cdot cm^2/s^{-1/2}$
Bare gold	32.0 (0.04)	356 (0.4)	138 (26)	1.6 (0.1) × 10^9
MCH	1.0 (0.35)	82 (47)	285 (60)	23 (10) × 10^6
CGG-8	0.04 (0.02)	6.4 (2.4)	3108 (193)	2750 (1508)
CCG-8	0.20 (0.05)	2.4 (0.2)	3128 (290)	1519 (437)
CTG-8	0.04 (0.01)	4.6 (0.6)	1497 (179)	514 (123)
CAG-8	0.19 (0.04)	6.0 (1.7)	1405 (183)	329 (741)
CAG-4	1.58 (0.80)	7.3 (5.9)	983 (98)	7 (4) × 10^6
GAA-8	0.07 (0.05)	2.5 (0.2)	1855 (75)	3312 (5312)
GAA-5	0.56 (0.15)	18.0 (5.4)	548 (54)	877 (625)
GAA-4	3.61 (0.69)	12.0 (2.6)	426 (70)	1219 (454)

Figure 1a shows representative curves of Nyquist form of EIS plots for dsTNR-8 sequences. The EIS plots for bare gold and MCH modified gold surfaces are given in supplementary information (**Figure S3**). In **Figure 1b-d**, R_{ct} compares number of variables between the groups and within the groups (green = highest, blue = medium, and red = least flexible groups). **Figure 1b** shows the comparison between representative dsTNR-8 sequences from three

flexibility groups. The results indicate that the CCG-8, representing the highest flexibility, has the largest R_{ct} than the medium and least flexible sequences. All three groups show distinct resistive

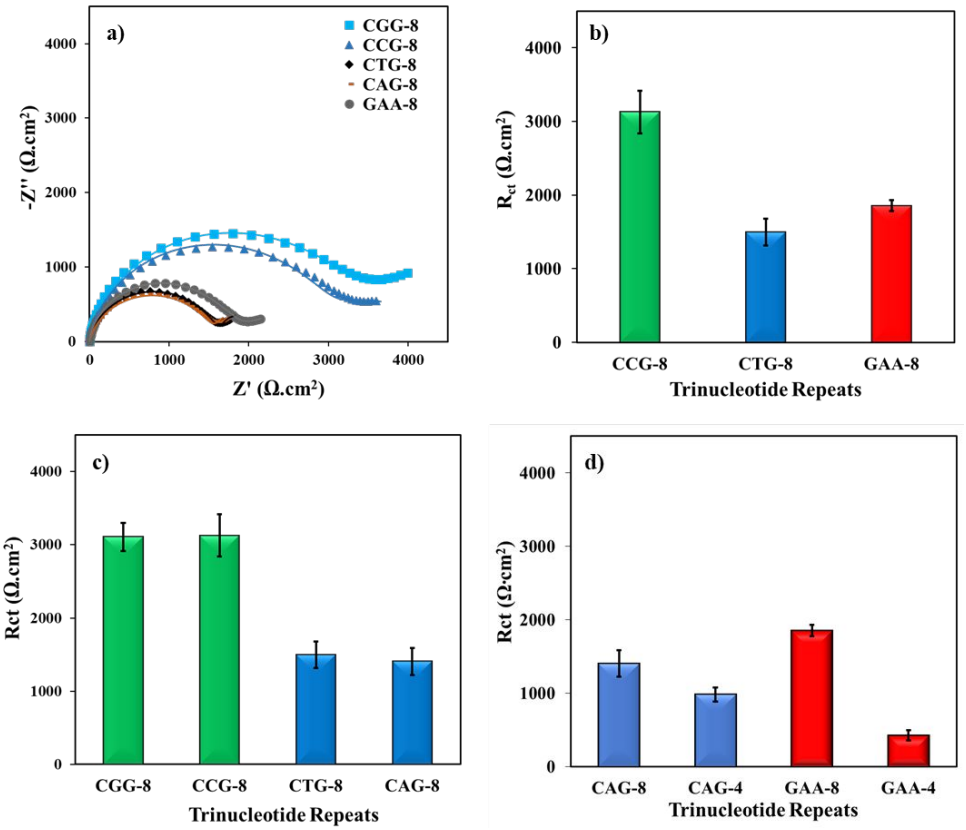

Figure 1. (a) Representative Nyquist form of EIS plots of dsTNR-8 from three flexibility groups. Markers show experimental data points and lines represent curve fits to modified Randle's equivalent circuit. (b) Comparing R_{ct} responses of representative dsTNR-8 sequences of three group, (c) comparing pairs of dsTNR-8 from highest and medium flexibility groups, (d) comparing two different lengths dsTNR-8 and dsTNR-4 from medium and least flexibility group. Green = highest flexibility, Blue = medium flexibility, and Red = least flexibility group. Error bars represent standard deviation of 4 replicate surfaces.

character but higher R_{ct} of GAA-8 (least flexible) than CTG-8 (medium flexible) indicates that the electrochemical resistive property is dependent on sequence context but independent of their rank in flexibility scale. One may assume that switching tethering strand in a duplex may cause change in the resistive property. To assess the effect of tethering strand, **Figure 1c** compares dsTNR-8 from highest flexibility and medium flexibility groups, where the pairs from each group are

complementary to each other, i.e. CGG vs. GCC and CTG vs. CAG with the difference of tethering strand. It is evident that R_{ct} responses of complementary TNR duplexes are indistinguishable from each other while the significant difference between the two groups still exists. This result suggests that for a biosensing application any strand from a duplex can be used for surface immobilization to observe overall resistive response of a repeat sequence. To investigate how the length of TNR of different flexibilities affects their resistive property, medium and least flexibility groups with 8 and 4 repeat units were compared in **Figure 1d**. The R_{ct} was lower for the shorter repeats in both groups due to less negative charge and physical resistance, however, the degree of change was much higher in case of least flexible GAA sequence (77% decrease) compared to medium flexible CAG (30% decrease). The results suggest that the degree of change in resistive properties with respect to length may also be sequence-dependent which perhaps affects their monolayer structure, uniformity, and packing.

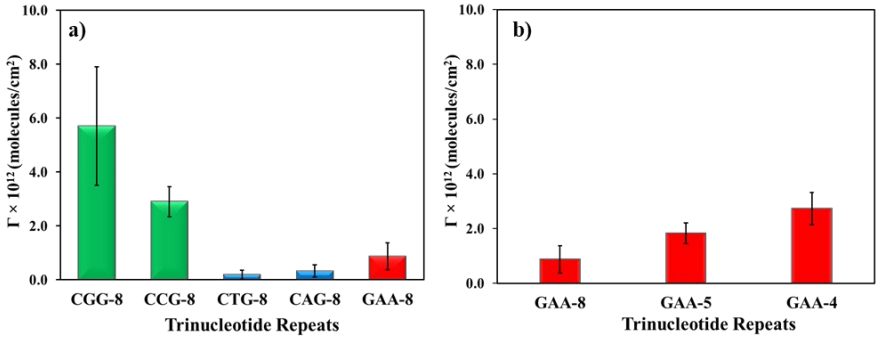

Figure 2. (a) Surface densities of dsTNR-8 sequences of three flexibility groups. (b) Surface densities of different lengths of dsGAA sequences. Green = highest flexibility, Blue = medium flexibility, and Red = least flexibility group. Error bars represent standard deviation of 4 replicate surfaces.

Surface coverage of TNRs may also be affected by their sequence context and flexibility. To investigate the effect, the surface densities were measured using Tarlov's method,[20] which

relies on the charge accumulation on DNA modified surface due to adsorption $Ru(NH_3)_6^{3+}$ on the phosphate groups of DNA film (see supplementary information for the details of the method). The accumulated charge is correlated to number of phosphate groups in the DNA monolayer and that can be converted into number of DNA strands immobilized using Cottrell equation. The results shown in **Figure 2a** prove that the surface coverage of three groups is distinguishable and affected by the type of a TNR sequence similarly as resistive property shown above. With respect to length, GAA with 4, 5, and 8 repeats was tested and the surface density was found decreasing with the length (**Figure 2b**), which is similar to a report on single-stranded DNA probe sequences.[28] **Table S1** in the supplementary information gives the surface density in number of strands ($\times 10^{12}$ molecules/cm^2), number of moles (pmol/cm^2), and the mass adsorbed (ng/cm^2) on the surface. Despite decrease in the surface density with length the R_{ct} for these sequences increased (see **Table 2**) confirming that the R_{ct} property is not only sensitive to coverage but also the length which affects the accumulation of charge at the DNA-electrode interface. Overall, the results suggest that the surface coverage is also a function of TNR sequence context, which can be significantly distinct for different TNRs of same length and for a specific TNR of different lengths.

Preparation of biocompatible films on ultra-flat gold surfaces provides detailed topographic characterization and electronic properties of the surface as recently achieved using single crystalline gold nanoplates.[29-30] To investigate if TNR sequence context or helical flexibility manifest into unique structure of the films, topographic images of dsTNR-8 films from three flexibility groups were obtained on ultra-flat gold surfaces (roughness RMS = 0.36 nm) using tapping mode AFM in air dry condition (**Figure 3**). Previously, AFM images were reported for surface-adsorbed strands of TNR sequences to study the molecular junctions in ~271 bp long sequence.[4] First time, this report compares topographic images of the TNR monolayers prepared

on ultra-flat gold substrates. All three sequences appear to be well-uniformed and closely packed as reported earlier for mixed-sequence double-stranded DNA oligonucleotides of similar length

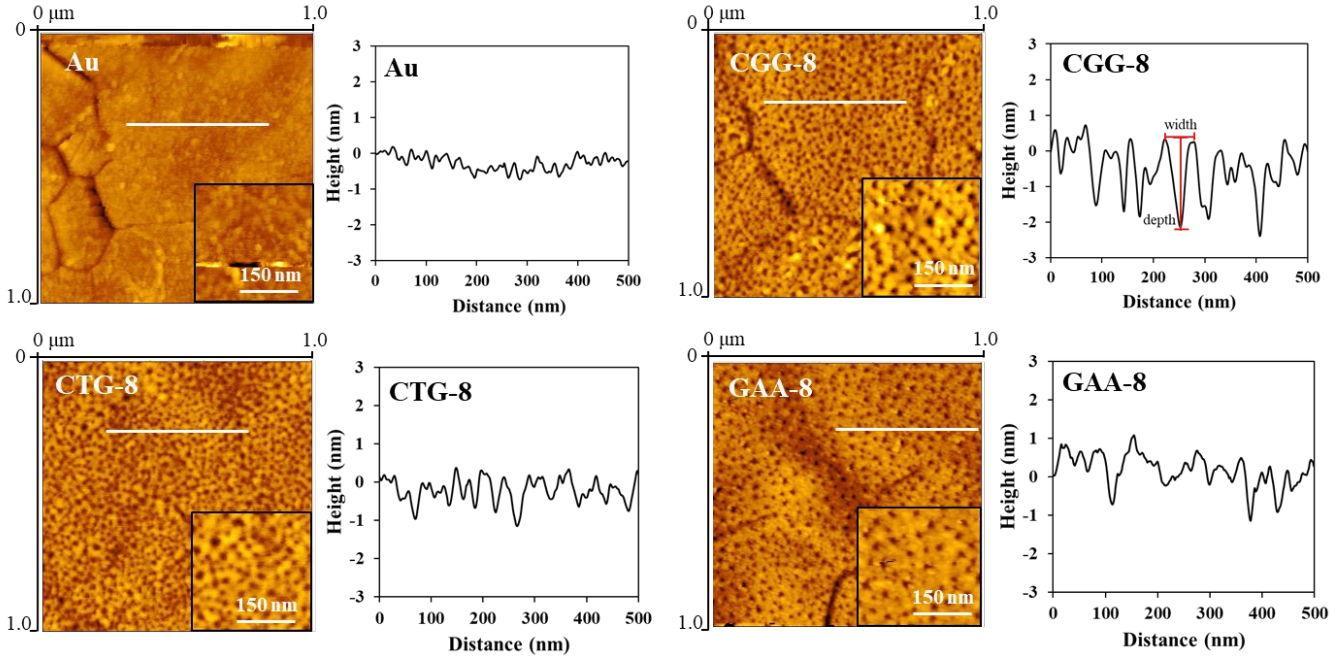

Figure 3. Tapping mode-AFM images of 1 µm × 1 µm area and line profile of bare ultra-flat gold substrate and surface-tethered films of double-stranded CGG-8, CTG-8, and GAA-8. White line in the images represents the region of extracted line profile of 500 nm length. The inset images in black borders are high resolution images (300 nm × 300 nm) of the surfaces. Black spots in the image are pinholes in TNR films and appear as inverted peaks in the extracted profiles. The red measurement lines in CGG-8 profile represents depth and width of an assumed pinhole. Height images are provided in the supplementary information.

and concentration.[31-32] Despite dense film packing the TNR molecules are protruding from the surface (as shown in the height image given in supplementary information **Figure S4**) with varying heights but lower than the theoretical height of an extended DNA duplex oriented normal to surface (~ 9 nm). The height profile suggests the approximate heights of CGG-8 (2.5 nm), CTG-8 (1.2 nm), and GAA-8 (1.8 nm), which also appears to sequence-specific rather than the rank in the flexibility scale. A unique feature which is clearly visible and comparable in the monolayer images is the size and density of pinholes (black spots), creating roughness on the surface compared to the

flat bare gold. By extracting the line profiles of each image across 500 nm length (white line), depth (roughness) and width of the so-called 'pinholes' were analysed as labelled on the line profile of CGG-8 (**Figure 3**). In addition, pinhole density (#pinholes/cm^2) was calculated by counting the number of pinholes using the images of 300 nm × 300 nm resolution given in the inset of each image in **Figure 3**. **Table 3** compares the parameters extracted from the surface profile, surface densities, and charge transfer resistance values of TNR-8 of three flexibility groups. Overall, the CGG-8 (highly flexible) has lower number of pinholes but highest roughness, pinhole width, surface density, and R_{ct}. In contrast, the medium flexible CTG-8 carries the highest number of pinholes but lowest roughness, pinhole width, surface density, and R_{ct}. The least flexible sequence of GAA-8 remains in between the two groups in all these properties. The extracted parameters from the topographic images confirm the sequence-dependence of the monolayer properties.

Table 3. The average values of surface parameters extracted from surface profile, surface densities, and charge transfer resistance values of dsTNR-8 of three flexibility groups. Parentheses represent standard deviation of measurements.

TNR	Flexibility	Number of Pinholes (cm^{-2})	Roughness/pinhole depth (nm)	Pinhole Width (nm)	Surface Density (10^{12} molecules/cm^2)	R_{ct} (Ω•cm^2)
CGG-8	Highest	1.0×10^{11}	2.3 (0.2)	46 (4)	5.7 (2.2)	3108 (193)
CTG-8	Medium	1.2×10^{11}	1.1 (0.1)	27 (4)	0.2 (0.1)	1497 (179)
GAA-8	Least	0.8×10^{11}	1.6 (0.2)	32 (4)	0.9 (0.5)	1855 (75)

Charge transport through DNA has been a hot area for nanoelectronics and bioelectronics application.[33-34] However, the challenge has been variety of factors profoundly affecting the DNA conductivity.[35] Probing electrical conductance of DNA has resulted in a variety of electrical behaviours, such as an insulator,[36-37] a semiconductor,[38-39] and a metal-like conductor.[40-41] Surface adsorbed DNA molecules with heights of ~2.4 nm were reported to be electrically conductive.[41] This was attributed to the fact that the height corresponds to diameter of B-DNA that may promote

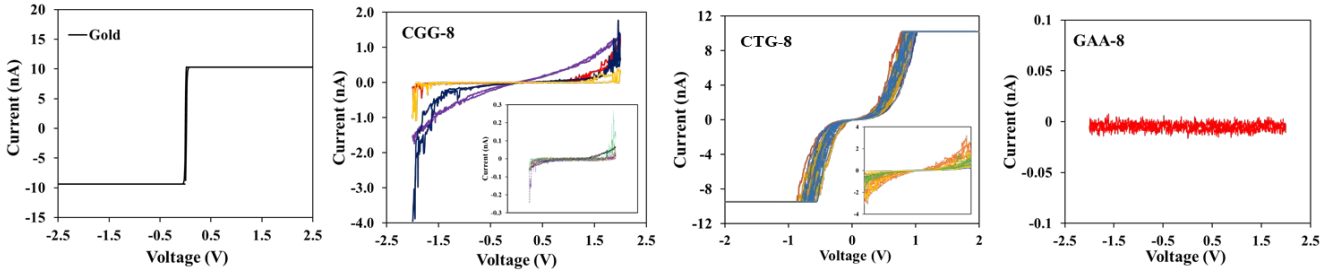

Figure 4. Current-voltage (*I-V*) curves of bare gold surface, double-stranded CGG-8, CTG-8 and GAA-8 repeats. The insets of CGG-8 and CTG-8 sequence show the lower current regime at pinholes of the sequence. At least five various spots were used to measure conductivity of these sequences.

charge transport through ordered π-stacked pathway. While, DNA molecules having 1.1 nm height behaved as insulators, perhaps due to the disruption of the B-DNA structure that diminishes the π-stack interactions between neighbouring base pairs. Further, DNA structures comprising long double strand, poly (G)-poly (C), tetra molecular G4-DNA molecules, chemically modified DNA, and hybrid metal-DNA complex were reported to be more conductive than bare dsDNA.[42] Here, we investigated the sequence-dependent effect of TNR on their electrical conductivity through C-AFM measurements in air using contact mode between ±2 V. **Figure 4** shows the *I-V* curves for bare gold substrate, dsCCG-8, dsCTG-8, and dsGAA-8 films. The gold substrate was found highly conductive where the current reached saturation to 10 nA as reported previously,[35] which confirms that the gold surface is highly clean and polished. To investigate conductivities of dsTNR-8, several loading forces were applied to make a contact between TNR and the tip using setpoint potentials 0.1 – 0.5 V (17–85 nN). This is because applying high force in the beginning may deform the films. The CGG-8 sequence was found to be non-conductive between 17–50 nN loading force and highly conductive like a gold substrate when applied beyond 68 nN force. Previously, Salmeron and co-workers observed a stepwise increase in current with applied loading force across 1-hexadecanethiol (~2 nm) monolayer on gold surface.[43] The same group also observed that the same load has different effect on the current response of different molecules due to different

adhesion force existing between the sample and tip.[44] In light of the past studies, we assume that a large adhesion force exists between the TNR samples and tip at loading force >68 nN that perhaps causes penetration through the monolayer and making a direct contact between the tip and gold substrate. Here, quantifying the effect of such contributing factors is beyond the scope of the work. After optimizing the loading force, 68 nN was set constant to collect *I-V* curves of TNR sequences. Previously, the similar strategy was used where dsDNA was chemically bonded to gold substrate but the contact between dsDNA and tip was physical which produced current less than 1 nA for similar length of sequences.[45] For CGG-8, the current was found higher than 1 nA at various spot (5 different spots) with slight differences. Moreover, one order of magnitude lower current was also observed around pinhole locations, shown in the inset of CGG-8, which is attributed to poor contact between the DNA and tip at those locations as observed previously.[45-46] Unexpectedly, CTG-8 was found to be 10× more conductive than CGG-8 with current >10 nA, while one order of magnitude lower currents were observed at pinhole locations as shown in the inset. These results are unexpected because such high current for such sequence, size, film height, and without a chemical bridge between tip and DNA have not been reported before. The electrical conductivity of CTG-8 is aligned with the electrochemical impedance response where the CTG-8 is least resistive than the other TNR-8. On the other hand, GAA-8 was found an insulator regardless the location of measurements. One reason may be it is an AT-rich sequence and it has been reported that the insertion of A-T basepairs into GC-rich sequences decrease conductance exponentially with the length of A-T basepairs with a decay constant of 0.43 $Å^{-1}$.[47] Nevertheless, the signature confirms the sequence-dependent conductive properties of the TNRs. It is important to note here that inhomogeneity and thus variance in electrical conduction of DNA films due to terraces and atomic steps of ultra-flat Au (111) surfaces, having roughness RMS ≈ 0.32 – 0.36 nm, has not been

a matter of concern in the previous reports.[31, 45, 48-49] We believe this is because of the large difference in the dimensions of DNA molecule and surface defects. Moreover, using a high concentration (e.g. 5-10 μM) and incubation time of 24-48 hours form a tightly packed film as shown **Figure 3**. Therefore, we ruled out this as a potential problem in our current measurements considering the present experimental conditions.

5. Conclusions.

We investigated here the effect of sequence context and flexibility of three disease-relevant trinucleotide repeat sequences on their monolayer properties. The sequences of three flexibility groups showed distinct electrochemical, electrical, and surface properties, which were found sequence-dependent rather than the reported flexibility rank. The trend of R_{ct} and surface densities were similar for the dsTNR-8, which shows a direct correlation between them. Nevertheless, the R_{ct} property was also found sensitive to length and charge of a DNA sequence, therefore, this property may be useful for designing a biosensing platform to detect few but very long repeat sequences. Topographically, it was clear that despite having same basepair lengths at molecular level, the surface-tethered films of repeats adopted unique structure directed by their sequence. The electrical conductance proved that the film height less than 2.4 nm can also be conductive without even a chemical bridge therefore sequence dependence may an appropriate parameter to explain the behaviour. Thus, the unique responses of the TNR studied here will be useful to design biosensing platforms for the fatal neurodegenerative diseases as well as give a new direction to bioelectronics field in future.

6. Conflicts of interest.

There are no conflicts to declare.

7. Acknowledgement.

Authors acknowledge Prof. Yi Lu from University of Illinois Urbana-Champaign. for his useful suggestions on the manuscript. We also acknowledge Dr. Kathy Walsh at Material Research Laboratory, University of Illinois at Urbana-Champaign Illinois. *"Atomic force microscopy image was carried out in part in the Materials Research Laboratory Central Research Facilities, University of Illinois."*

8. References.

1. Mitas, M., Trinucleotide repeats associated with human disease. *Nucleic Acids Res* **1997,** *25* (12), 2245-2254.
2. Rohilla, K. J.; Gagnon, K. T., RNA biology of disease-associated microsatellite repeat expansions. *Acta Neuropathologica Communications* **2017,** *5* (1), 63.
3. Kiliszek, A.; Rypniewski, W., Structural studies of CNG repeats. *Nucleic Acids Res* **2014,** *42* (13), 8189-8199.
4. Sinden, R. R.; Potaman, V. N.; Oussatcheva, E. A.; Pearson, C. E.; Lyubchenko, Y. L.; Shlyakhtenko, L. S., Triplet repeat DNA structures and human genetic disease: dynamic mutations from dynamic DNA. *Journal of Biosciences* **2002,** *27* (1), 53-65.
5. Baldi, P.; Baisnee, P. F., Sequence analysis by additive scales: DNA structure for sequences and repeats of all lengths. *Bioinformatics* **2000,** *16* (10), 865-89.
6. Gellibolian, R.; Bacolla, A.; Wells, R. D., Triplet repeat instability and DNA topology: an expansion model based on statistical mechanics. *J Biol Chem* **1997,** *272* (27), 16793-7.
7. Chastain, P. D.; Sinden, R. R., CTG repeats associated with human genetic disease are inherently flexible. *J Mol Biol* **1998,** *275* (3), 405-11.
8. Gomes-Pereira, M.; Monckton, D. G., Ethidium Bromide Modifies The Agarose Electrophoretic Mobility of CAG.CTG Alternative DNA Structures Generated by PCR. *Frontiers in Cellular Neuroscience* **2017,** *11*.

9. Chastain, P. D.; Eichler, E. E.; Kang, S.; Nelson, D. L.; Levene, S. D.; Sinden, R. R., Anomalous Rapid Electrophoretic Mobility of DNA Containing Triplet Repeats Associated with Human Disease Genes. *Biochemistry-Us* **1995,** *34* (49), 16125-16131.
10. Malgowska, M.; Gudanis, D.; Kierzek, R.; Wyszko, E.; Gabelica, V.; Gdaniec, Z., Distinctive structural motifs of RNA G-quadruplexes composed of AGG, CGG and UGG trinucleotide repeats. *Nucleic Acids Res* **2014,** *42* (15), 10196-10207.
11. Sobczak, K.; Michlewski, G.; de Mezer, M.; Kierzek, E.; Krol, J.; Olejniczak, M.; Kierzek, R.; Krzyzosiak, W. J., Structural Diversity of Triplet Repeat RNAs. *Journal of Biological Chemistry* **2010,** *285* (17), 12755-12764.
12. Zheng, M.; Huang, X.; Smith, G. K.; Yang, X.; Gao, X., Genetically Unstable CXG Repeats are Structurally Dynamic and Have a High Propensity for Folding. An NMR and UV Spectroscopic Study. *Journal of molecular biology* **1996,** *264* (2), 323-336.
13. Huang, X. N.; Gao, X. L., *Toward the understanding of the molecular basis of triplet expansion. Studies of the single stranded CCG and CGG DNA trinucleotide repeats by NMR*. 1998; p 221-234.
14. Paiva, A. M.; Sheardy, R. D., Influence of Sequence Context and Length on the Structure and Stability of Triplet Repeat DNA Oligomers. *Biochemistry* **2004,** *43* (44), 14218-14227.
15. Huang, J.; Delaney, S., Unique Length-Dependent Biophysical Properties of Repetitive DNA. *The Journal of Physical Chemistry B* **2016,** *120* (18), 4195-4203.
16. Qamar, A. Z.; Asefifeyzabadi, N.; Taki, M.; Naphade, S.; Ellerby, L. M.; Shamsi, M. H., Characterization and application of fluidic properties of trinucleotide repeat sequences by wax-on-plastic microfluidics. *Journal of Materials Chemistry B* **2020,** *8* (4), 743-751.
17. Rao, A. N.; Grainger, D. W., BIOPHYSICAL PROPERTIES OF NUCLEIC ACIDS AT SURFACES RELEVANT TO MICROARRAY PERFORMANCE. *Biomater Sci* **2014,** *2* (4), 436-471.
18. Taki, M.; Rohilla, K. J.; Barton, M.; Funneman, M.; Benzabeh, N.; Naphade, S.; Ellerby, L. M.; Gagnon, K. T.; Shamsi, M. H., Novel probes for label-free detection of neurodegenerative GGGGCC repeats associated with amyotrophic lateral sclerosis. *Anal Bioanal Chem* **2019,** *411* (26), 6995-7003.

19. Au, L.; Lim, B.; Colletti, P.; Jun, Y.-S.; Xia, Y., Synthesis of Gold Microplates Using Bovine Serum Albumin as a Reductant and a Stabilizer. *Chemistry – An Asian Journal* **2010,** *5* (1), 123-129.
20. Steel, A. B.; Herne, T. M.; Tarlov, M. J., Electrochemical Quantitation of DNA Immobilized on Gold. *Analytical Chemistry* **1998,** *70* (22), 4670-4677.
21. http://gwyddion.net/.
22. Jithesh, P. V.; Singh, P.; Joshi, R., Molecular dynamics studies of trinucleotide repeat DNA involved in neurodegenerative disorders. *Journal of biomolecular structure & dynamics* **2001,** *19* (3), 479-95.
23. Kafka, J.; Pänke, O.; Abendroth, B.; Lisdat, F., A label-free DNA sensor based on impedance spectroscopy. *Electrochim Acta* **2008,** *53* (25), 7467-7474.
24. Alam, M. N.; Shamsi, M. H.; Kraatz, H.-B., Scanning positional variations in single-nucleotide polymorphism of DNA: an electrochemical study. *Analyst* **2012,** *137* (18), 4220-4225.
25. Shamsi, M. H.; Kraatz, H.-B., Electrochemical signature of mismatch in overhang DNA films: a scanning electrochemical microscopic study. *The Analyst* **2013,** *138* (12), 3538-3543.
26. Shamsi, M. H.; Kraatz, H.-B., The effects of oligonucleotide overhangs on the surface hybridization in DNA films: an impedance study. *Analyst* **2011,** *136* (15), 3107-3112.
27. Riedel, M.; Kartchemnik, J.; Schöning, M. J.; Lisdat, F., Impedimetric DNA Detection—Steps Forward to Sensorial Application. *Anal Chem* **2014,** *86* (15), 7867-7874.
28. Steel, A. B.; Levicky, R. L.; Herne, T. M.; Tarlov, M. J., Immobilization of Nucleic Acids at Solid Surfaces: Effect of Oligonucleotide Length on Layer Assembly. *Biophysical Journal* **2000,** *79* (2), 975-981.
29. Yoo, Y.; Lee, H.; Lee, H.; Lee, M.; Yang, S.; Hwang, A.; Kim, S.-i.; Park, J. Y.; Choo, J.; Kang, T.; Kim, B., Surfactant-Free Vapor-Phase Synthesis of Single-Crystalline Gold Nanoplates for Optimally Bioactive Surfaces. *Chemistry of Materials* **2017,** *29* (20), 8747-8756.
30. Jeong, W.; Lee, M.; Lee, H.; Lee, H.; Kim, B.; Park, J. Y., Ultraflat Au nanoplates as a new building block for molecular electronics. *Nanotechnology* **2016,** *27* (21), 215601.

31. Nogues, C.; Cohen, S. R.; Daube, S. S.; Naaman, R., Electrical properties of short DNA oligomers characterized by conducting atomic force microscopy. *Physical Chemistry Chemical Physics* **2004,** *6* (18), 4459-4466.
32. Erts, D.; Polyakov, B.; Olin, H.; Tuite, E., Spatial and mechanical properties of dilute DNA monolayers on gold imaged by AFM. *The Journal of Physical Chemistry B* **2003,** *107* (15), 3591-3597.
33. Korol, R.; Segal, D., From Exhaustive Simulations to Key Principles in DNA Nanoelectronics. *The Journal of Physical Chemistry C* **2018,** *122* (8), 4206-4216.
34. Genereux, J. C.; Barton, J. K., Mechanisms for DNA charge transport. *Chem Rev* **2010,** *110* (3), 1642-1662.
35. Jiménez-Monroy, K. L.; Renaud, N.; Drijkoningen, J.; Cortens, D.; Schouteden, K.; van Haesendonck, C.; Guedens, W. J.; Manca, J. V.; Siebbeles, L. D. A.; Grozema, F. C.; Wagner, P. H., High Electronic Conductance through Double-Helix DNA Molecules with Fullerene Anchoring Groups. *The Journal of Physical Chemistry A* **2017,** *121* (6), 1182-1188.
36. de Pablo, P. J.; Moreno-Herrero, F.; Colchero, J.; Gómez Herrero, J.; Herrero, P.; Baró, A. M.; Ordejón, P.; Soler, J. M.; Artacho, E., Absence of dc-Conductivity in $\ensuremath{\lambda}$-DNA. *Physical Review Letters* **2000,** *85* (23), 4992-4995.
37. Storm, A. J.; Noort, J. v.; Vries, S. d.; Dekker, C., Insulating behavior for DNA molecules between nanoelectrodes at the 100 nm length scale. *Applied Physics Letters* **2001,** *79* (23), 3881-3883.
38. Porath, D.; Bezryadin, A.; de Vries, S.; Dekker, C., Direct measurement of electrical transport through DNA molecules. *Nature* **2000,** *403* (6770), 635-8.
39. Watanabe, H.; Manabe, C.; Shigematsu, T.; Shimotani, K.; Shimizu, M., Single molecule DNA device measured with triple-probe atomic force microscope. *Applied Physics Letters* **2001,** *79* (15), 2462-2464.
40. Murphy, C. J.; Arkin, M. R.; Jenkins, Y.; Ghatlia, N. D.; Bossmann, S. H.; Turro, N. J.; Barton, J. K., Long-range photoinduced electron transfer through a DNA helix. *Science* **1993,** *262* (5136), 1025-9.

41. Kasumov, A. Y.; Klinov, D. V.; Roche, P.-E.; Guéron, S.; Bouchiat, H., Thickness and low-temperature conductivity of DNA molecules. *Applied Physics Letters* **2004,** *84* (6), 1007-1009.
42. Zhuravel, R.; Stern, A.; Fardian-Melamed, N.; Eidelshtein, G.; Katrivas, L.; Rotem, D.; Kotlyar, A. B.; Porath, D., Advances in Synthesis and Measurement of Charge Transport in DNA-Based Derivatives. *Adv Mater* **2018,** *30* (41), 1706984.
43. Qi, Y.; Ratera, I.; Park, J. Y.; Ashby, P. D.; Quek, S. Y.; Neaton, J. B.; Salmeron, M., Mechanical and Charge Transport Properties of Alkanethiol Self-Assembled Monolayers on a Au(111) Surface: The Role of Molecular Tilt. *Langmuir* **2008,** *24* (5), 2219-2223.
44. Fang, L.; Park, J. Y.; Ma, H.; Jen, A. K. Y.; Salmeron, M., Atomic Force Microscopy Study of the Mechanical and Electrical Properties of Monolayer Films of Molecules with Aromatic End Groups. *Langmuir* **2007,** *23* (23), 11522-11525.
45. Cohen, H.; Nogues, C.; Ullien, D.; Daube, S.; Naaman, R.; Porath, D., Electrical characterization of self-assembled single- and double-stranded DNA monolayers using conductive AFM. *Faraday Discussions* **2006,** *131* (0), 367-376.
46. Salomon, A.; Cahen, D.; Lindsay, S.; Tomfohr, J.; Engelkes, V. B.; Frisbie, C. D., Comparison of electronic transport measurements on organic molecules. *Advanced Materials* **2003,** *15* (22), 1881-1890.
47. Xu; Zhang; Li; Tao, Direct Conductance Measurement of Single DNA Molecules in Aqueous Solution. *Nano Letters* **2004,** *4* (6), 1105-1108.
48. Cai, L.; Tabata, H.; Kawai, T., Probing electrical properties of oriented DNA by conducting atomic force microscopy. *Nanotechnology* **2001,** *12* (3), 211-216.
49. Cohen, H.; Nogues, C.; Naaman, R.; Porath, D., Direct measurement of electrical transport through single DNA molecules of complex sequence. *Proc Natl Acad Sci U S A* **2005,** *102* (33), 11589-93.

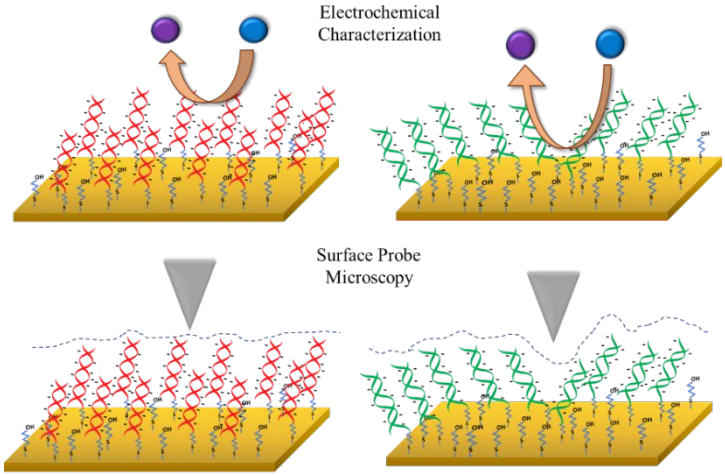

Sequence-dependent properties of the surface-assembled trinucleotide repeat interface on gold surface were explored by electrochemical methods and surface probe microscopy.